ANL/CMT/CP-96586

# METAL WASTE FORMS FROM TREATMENT OF EBR-II SPENT FUEL*

Daniel P. Abraham, Dennis D. Keiser, Jr., Sean M. McDeavitt

Argonne National Laboratory
Chemical Technology Division
Nuclear Technology Program
9700 South Cass Avenue
Argonne, IL 60439
Ph: (630) 252-4332
Fax: (630) 252-5246
E-mail: abraham@cmt.anl.gov



To be presented at the Spectrum '98 Conference
Denver, CO
September 13-18, 1998



*Work supported by the U.S. Department of Energy, Nuclear Energy Research & Development Program, under Contract W-31-109-ENG-38.

## DISCLAIMER

# METAL WASTE FORMS FROM TREATMENT OF EBR-II SPENT FUEL

Daniel P. Abraham
Argonne National Laboratory
9700 South Cass Avenue
Argonne, Illinois 60439
(630) 252-4332

Dennis D. Keiser, Jr.
Argonne National Laboratory(W)
P. O. Box 2528
Idaho Falls, Idaho 83403
(208) 533-7298

Sean M. McDeavitt
Argonne National Laboratory
9700 South Cass Avenue
Argonne, Illinois 60439
(630) 252-4308

## ABSTRACT

Demonstration of Argonne National Laboratory's electrometallurgical treatment of spent nuclear fuel is currently being conducted on irradiated, metallic driver fuel and blanket fuel elements from the Experimental Breeder Reactor-II (EBR-II) in Idaho. The residual metallic material from the electrometallurgical treatment process is consolidated into an ingot, the metal waste form (MWF), by employing an induction furnace in a hot cell. Scanning electron microscopy (SEM) and chemical analyses have been performed on irradiated cladding hulls from the driver fuel, and on samples from the alloy ingots. This paper presents the microstructures of the radioactive ingots and compares them with observations on simulated waste forms prepared using non-irradiated material. These simulated waste forms have the baseline composition of stainless steel - 15 wt % zirconium (SS-15Zr). Additions of noble metal elements, which serve as surrogates for fission products, and actinides are made to that baseline composition. The partitioning of noble metal and actinide elements into alloy phases and the role of zirconium for incorporating these elements is discussed in this paper.

## I. INTRODUCTION

An electrometallurgical treatment process that separates uranium from other nuclear fuel constituents is currently being demonstrated using metallic spent nuclear fuel from the Experimental Breeder Reactor-II (EBR-II) reactor located at the Argonne National Laboratory West (ANL-W) site in Idaho [1]. This demonstration is being performed in the Fuel Conditioning Facility (FCF) using 100 driver fuel assemblies and 25 blanket fuel assemblies from EBR-II. The driver elements are composed of uranium-10 wt% zirconium (U-10Zr) alloy fuel and Type 316 or D9 stainless steel (SS) cladding. The blanket elements comprise uranium metal and Type 304SS cladding.

In the electrometallurgical process, chopped driver or blanket fuel segments are placed into the anode baskets of an electrorefiner. When a potential is applied, uranium, active fission products and transuranic (TRU) elements dissolve at the anode into the molten salt electrolyte, while uranium is deposited onto a steel cathode [2]. The active fission products and TRU elements in the molten salt are extracted by contacting the salt with anhydrous zeolite. The loaded zeolite is mixed with glass frit and hot pressed to make a ceramic waste form [3]. The irradiated fuel cladding, assembly hardware, zirconium from the alloy fuel, noble metal fission products (e.g., Tc, Rh, Ru, Pd, and Nb), and small amounts of actinides left behind in the anodic dissolution baskets are melted together to make a metal waste form (MWF). Both the ceramic and metal waste forms are intended for disposal in a geologic repository [3].

The baseline metal waste form selected for the EBR-II fuels is the SS-15Zr alloy [4]. Simulated waste forms using non-irradiated materials have been produced and tested at the ANL-East (ANL-E) site in Chicago. The alloy microstructure, corrosion behavior, and mechanical and thermophysical properties have been characterized on these non-radioactive samples [5]. The results indicate that the alloy is an excellent waste form that will be very durable under the conditions expected in the planned repository at Yucca Mountain, NV. Tests on SS-15Zr alloys containing Tc and actinide additions

have shown that the waste form is also resistant to selective leaching of these elements.

The noble metal fission product (NMFP) content of the MWF will range from 0.5 to 4 wt %, depending upon the burnup of the spent fuel [6]. We will discuss the partitioning of NMFPs in the major phases of the SS-15Zr alloy. Microstructures of alloys containing 0, 5 and 15 wt % Zr will be presented to highlight the role of zirconium in NMFP distribution in the various alloy phases. Microstructures of a U-bearing sample will be used to show actinide distribution in the SS-15Zr alloy. Analyses of irradiated cladding hulls used to make actual waste form ingots will be presented. Finally, microstructures from the actual waste form ingots will be compared with those observed in the simulated waste forms.

## II. EXPERIMENTAL

Non-radioactive samples generated to study noble metal distribution were produced in a tungsten-element furnace using stainless steel, zirconium, and high-purity noble metal elements. The radioactive samples, which contained Tc and depleted U (DU), were generated in a resistance furnace within a hot cell. The Tc used in the cast samples was produced by heating ammonium pertechnetate to 900°C in a hydrogen atmosphere. The starting materials for all ingots were placed in a yttrium oxide crucible and melted at 1600°C in an argon atmosphere. The resulting alloy was allowed to solidify, either within the crucible, or after being poured into a casting mold. Alloy specimens were sectioned from the solidified ingots, prepared for microstructural examination, and studied with a JEOL 6400 scanning electron microscope with an Energy Dispersive Spectroscopy (EDS) attachment from NORAN instruments. The crystal structure of phases in the SS-15Zr alloy was determined from neutron diffraction data collected at the Intense Pulsed Neutron Source (IPNS) located at ANL-E.

Metal waste form ingots from irradiated cladding hulls were cast using both vacuum induction and resistance furnaces located in an argon hot cell. The electrorefiner LiCl-KCl eutectic salt adhering to the cladding hulls was first volatilized at 1100°C in a distillation furnace. The salt-free hulls were placed in yttrium oxide crucibles, along with enough Zr metal to make up the nominal SS-15Zr composition, and heated to 1600°C in an argon atmosphere. The resulting ingots were cooled within the yttrium oxide crucibles. The ingots were sampled by injection-casting, where molten alloy is vacuum-injected into a zirconia-mold-washed quartz tube, or by core-drilling with a diamond-tipped, 0.5 in. (1.27 cm) dia. drill bit.

Irradiated hull samples, ~0.25 in. (0.635 cm) long x 0.230 in. (0.584 cm) dia., were selected at various stages of the process for SEM examination. Some samples were taken directly after electrorefining but before the salt distillation step; others were chosen after salt distillation but before the ingot consolidation step. The samples taken after electrorefining were washed with water implemented to remove the adhering salt. Removing the salt lowered the radioactivity of the samples, thereby minimizing the negative effects on the EDS detector (e.g., peak broadening, high background noise, high dead times, etc.). Microstructural examination was performed on gold-coated specimens using an ETEC Autoscan scanning electron microscope equipped with a Kevex 8000 (Fisons Instruments) energy dispersive X-ray analysis system. Irradiated hull samples were also chemically analyzed to determine the amount of U and Zr left behind after the electrorefining step.

## III. RESULTS AND DISCUSSION

### A. Noble Metal and Actinide Partitioning in SS-15Zr Alloy

A typical microstructure of as-cast SS-15Zr contains a mixture of coarse and fine eutectics. (see Fig.1). The major phases in the alloy microstructure are ferrite, an iron-rich solid solution phase, and a Laves intermetallic $Zr(Fe,Cr,Ni)_{2+x}$ [7]. Small amounts (<10 vol%) of austenite, another iron-rich solid solution phase, and the $(Fe,Cr,Ni)_{23}Zr_6$ intermetallic (< 5 vol%) are also present in the alloy [8]. The distribution of NMFPs in SS-15Zr alloy phases was investigated through the addition of representative elements, such as Ru, Tc, Pd, Ag and Nb. Noble metal additions were made in combinations that totaled ~4 wt % per sample. For example, a typical noble metal addition to a SS-15Zr alloy was 2 Ru-1.5 Pd-0.5 Ag.. The

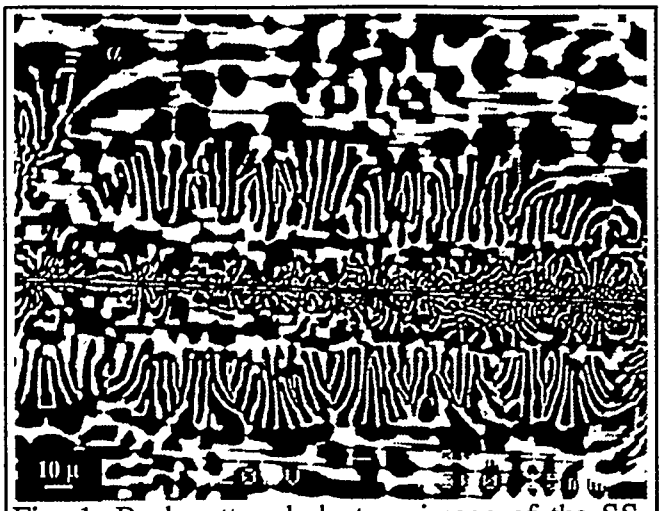

Fig. 1. Backscattered electron image of the SS-15Zr alloy microstructure. The bright phase is the $Zr(Fe,Cr,Ni)_{2+x}$ intermetallic; the dark phase is ferrite.

amounts of individual noble metal were often much higher than expected levels in "real" waste forms, but the elevated concentrations were necessary to enable accurate detection by EDS.

A summary of elemental distribution in the major SS-15Zr alloy phases is shown in Table 1. Some of the noble metals (Tc, Re, Co, Mo, Mn and W) are evenly distributed throughout the SS-15Zr alloy, while others (Ru, Nb, Pd, Sn, Si, Ag and Ta) are concentrated in the intermetallic phases. In all cases, the noble metals were soluble in the alloy phases at representative waste form concentrations. The absence of discrete noble metal phases suggests that the fission product release rate from the SS-15Zr alloy will be controlled by the corrosion behavior of the alloy matrix phases.

The distribution of actinides (mainly U) in the metal waste form is of interest because small amounts of actinide elements are present in the metal waste stream. The microstructure of SS-15Zr alloy containing 5 wt % DU is shown in Fig. 2. In addition to the iron-rich solid solution phases and the $Zr(Fe,Cr,Ni)_{2+x}$ intermetallic, uranium-rich regions are observed within the $Zr(Fe,Cr,Ni)_{2+x}$ intermetallic. The volume fraction of these uranium-rich regions increases with the uranium content of the alloy. Similar actinide-rich regions were also observed in alloys containing Pu and Np [9]. Neutron diffraction studies on a SS-15Zr-5DU alloy are currently

Table 1. Distribution of Noble Metals in the Major Phases of the SS-15Zr Alloy

| Element | Ratio of element in the Intermetallic to that in the Iron solid solutions* |
|---|---|
| Ag | 5:1 |
| Co | 1 : 1 |
| Mn | < 1 : 1 |
| Mo | < 1 : 1 |
| Nb | 8 : 1 |
| Pd | 10 : 1 |
| Re | 1 : 1 |
| Ru | 4 : 1 |
| Si | 9 : 1 |
| Sn | 9 : 1 |
| Ta | 8 : 1 |
| Tc | 1 : 1 |
| W | 1 : 1 |

* Ratios are approximate (±50%), especially for the larger numbers.

underway to determine the nature and crystal structure of these actinide-rich regions.

B. Role of Zr in the Incorporation of NMFPs

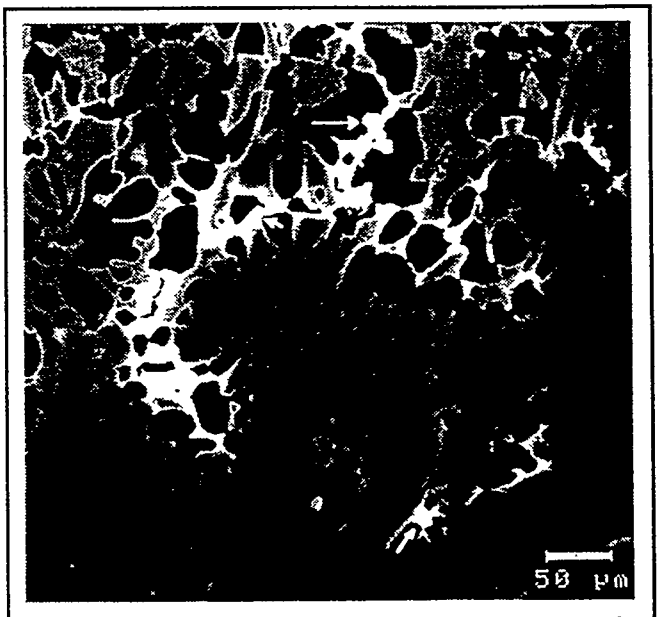

Fig. 2. Backscattered electron micrograph of a SS-15Zr-5DU alloy. The dark phase is ferrite. The high-contrast regions (indicated by arrows) within the $Zr(Fe,Cr,Ni)_{2+x}$ intermetallic are rich in uranium.

Noble metal distribution was studied in stainless steel alloys that contained 5 wt % and 0 wt % Zr to determine the effect of Zr content on MWF microstructure. Fig. 3 shows the typical microstructure of a 5 wt % Zr alloy with Ag, Pd and Ru. Compared to a SS-15Zr alloy, the 5 wt % Zr alloy contains less $Zr(Fe,Cr,Ni)_{2+x}$ and more austenite and ferrite. Negligible amounts of Ag and Pd are present in the iron solid solution phases, austenite and ferrite. Some Ag (~ 0.6 at %) is dissolved in $Zr(Fe,Cr,Ni)_{2+x}$, but the majority of the element appears as a separate phase (see Fig. 3). Pd-rich areas within the $Zr(Fe,Cr,Ni)_{2+x}$ intermetallic are also seen in Fig. 3. The $Zr(Fe,Cr,Ni)_{2+x}$ intermetallic has a higher solubility for Pd and can dissolve ~ 5.7 at %; Pd-rich areas form only after $Zr(Fe,Cr,Ni)_{2+x}$ is saturated with the element. Distinct Ru-rich areas were not observed in the alloy. Ruthenium is present in all phases but shows a preference for $Zr(Fe,Cr,Ni)_{2+x}$.

In stainless steel alloys without zirconium, a complex mixture of stainless steel phases, noble metal-rich solid solution phases, and intermetallic phases are observed. The $Zr(Fe,Cr,Ni)_{2+x}$ intermetallic does not form because the alloy contains no zirconium. The typical microstructure of a stainless steel alloy with Ag, Pd, Ru and Nb is shown in Fig. 4. The various phases and their relative proportions in this alloy are as follows: (1) austenite matrix (dominant), (2) ferrite (minor), (3) silver-rich phase (minor), (4) niobium-rich phase (minor), (5) a Mo-Mn intermetallic (very minor) and (6) a Nb-rich intermetallic (very minor).

Zirconium plays a crucial role in the incorporation of fission products into the MWF microstructure. In the absence of zirconium, NMFP elements in stainless steel alloys precipitate into fission product-rich phases. The addition of zirconium to stainless steel results in the formation of $Zr(Fe,Cr,Ni)_{2+x}$ intermetallics, which are the preferred sites for several noble metals. Fission product incorporation in alloy phases is strongly influenced by the volume fraction of $Zr(Fe,Cr,Ni)_{2+x}$, which is in turn influenced by the zirconium content of the alloy. Noble metal-rich phases appear only when the $Zr(Fe,Cr,Ni)_{2+x}$ intermetallics are saturated with the elements. Such phases are more prominent in alloys with less than 15 wt % Zr because of their lower $Zr(Fe,Cr,Ni)_{2+x}$ content.

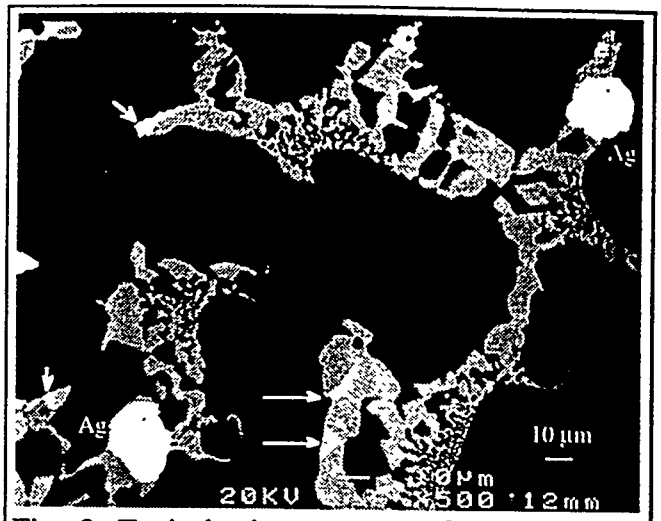

Fig. 3: Typical microstructure of a 316SS-5Zr-0.5Ag-1.5Pd-2Ru alloy. Silver-rich areas and Pd-rich regions in the intermetallic (marked by arrows) are visible. The dark areas contain the iron-rich phases austenite and ferrite.

C. Analysis of Irradiated Cladding Hulls

The fuel cladding makes up a large fraction (> 80%) of the metal waste stream. Small tubular segments of the cladding called "cladding hulls" were examined to determine the nature of this material. Layers rich in zirconium were observed on both inner and outer surfaces of the cladding hulls. These layers were present in samples taken directly from the electrorefiner (Fig. 5) and on the samples obtained after salt distillation (Fig. 6). Apparently, Zr metal (with minor amounts of U) is deposited on the cladding

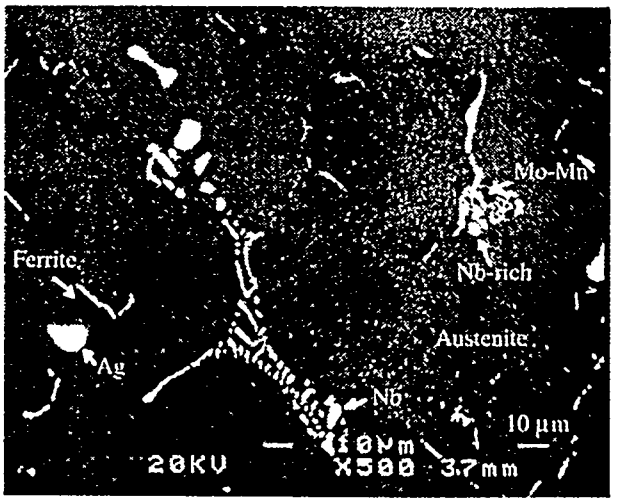

Fig. 4: Typical microstructure of a 316SS-0.5Ag-1Nb-1Pd-1.5Ru (no Zr) alloy.

hulls during the electrorefining process [8]. When the hulls are heated to 1100°C in the salt-distillation furnace, interdiffusion between the Zr metal and the cladding components (e.g., Fe, Cr and Ni) results in the formation of intermetallic phases. Elemental analyses indicate that these intermetallics are similar to $Zr(Fe,Cr,Ni)_{2+x}$, but they also contain some U. The presence of these multiphase diffusion structures does not impede the melting and consolidation of the cladding hulls.

D. Waste Form Ingots from Irradiated Hulls

The photograph of a typical waste form ingot produced in the FCF using irradiated cladding hulls is shown in Fig. 7. The ingot weighed ~ 5.6 kg and was ~ 7.75 in. (19.685 cm) in diameter and 1.5 in. (3.81 cm) high. Macroscopically, the ingot appeared homogeneous and well-consolidated. A sample was injection-cast from the ingot when the charge was molten. An SEM micrograph of the sample microstructure is presented in Fig. 8. It shows the two major phases observed in the SS-15Zr alloy. High-contrast regions observed within the intermetallic are similar to those seen in the SS-15Zr-5DU sample (Fig. 2). Chemical analysis of the hulls used to generate the ingot showed that the material contained 8.1 wt% Zr and 15.6 wt% U. The high-contrast regions are believed to be U-rich regions within the $Zr(Fe,Cr,Ni)_{2+x}$ intermetallic. Detailed analysis of alloy phases is continuing.

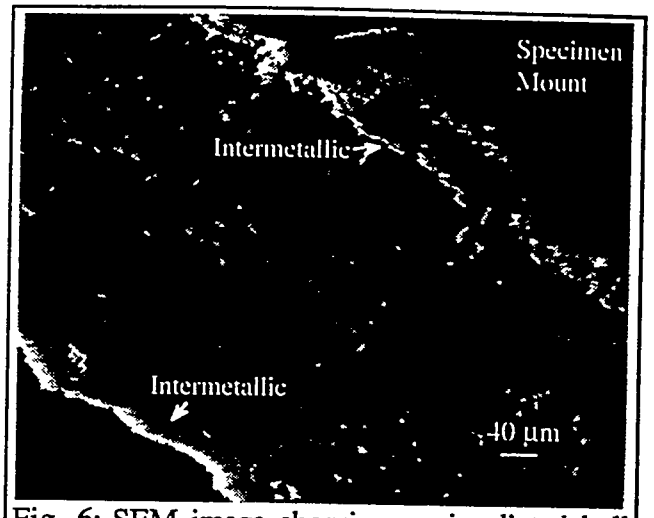

Fig. 6: SEM image showing an irradiated hull after salt-distillation. An intermetallic appears as a bright-contrast layer on the inner and outer circumference of the cladding hull. Other intermetallic phases appear in the hull interior.

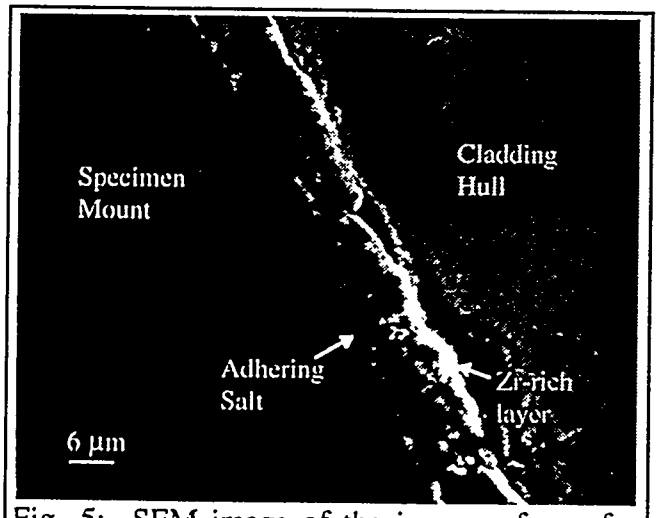

Fig. 5: SEM image of the inner surface of a water-washed, irradiated hull taken from the electrorefiner. The adhering salt and Zr-rich layer are clearly visible.

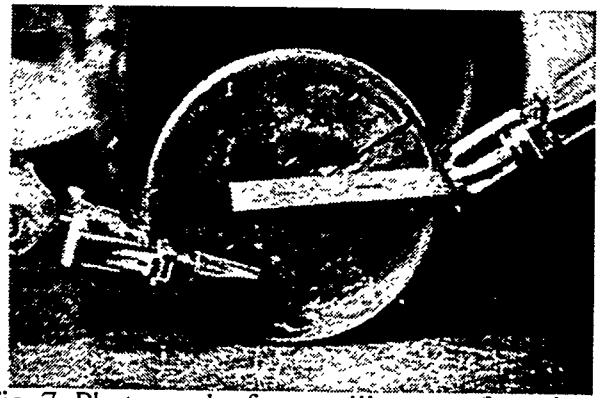
Fig. 7: Photograph of a metallic waste form ingot prepared from irradiated stainless steel cladding and added Zr.

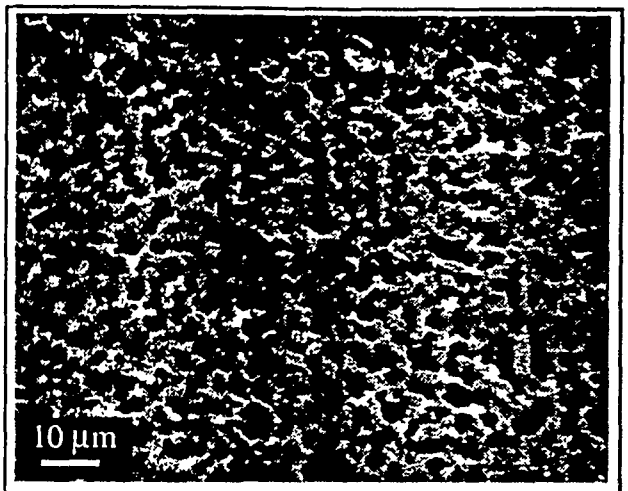


Fig. 8. SEM image of an injection-cast pin produced from an FCF ingot. The pin contains 15.6 wt % U and 8.1 wt % Zr.

The microstructure of another MWF ingot, produced from the same electrorefiner batch of cladding hulls used to generate the ingot in Fig. 7, is shown in Fig. 9. Some non-radioactive stainless steel was added to the cladding hulls before the hulls were consolidated. The final alloy had ~5 wt % Zr. The microstructure was obtained from a sample that was core-drilled from the ingot. The sample microstructure is very similar to that of simulated waste forms containing 5 wt % Zr. High-contrast regions similar to those seen in Fig. 8 were also observed in this alloy. These regions are believed to be areas enriched in U.

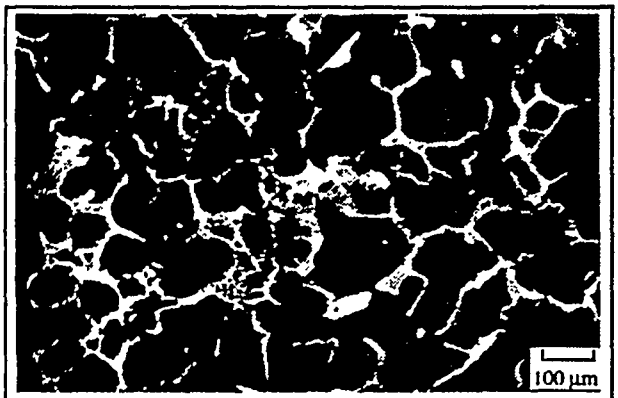


Fig. 9. SEM image showing an ingot with ~5 wt % Zr. The high contrast regions are believed to be enriched in uranium.

## V. SUMMARY AND CONCLUSIONS

Metal waste form ingots, using irradiated cladding hulls from EBR-II spent fuel, have been produced in the FCF. The radioactive ingots have been sampled and analyzed by SEM and chemical analyses techniques. Complementary work to determine the properties of the waste form alloy has been performed using non-irradiated materials. The conclusions of our study are as follows:

(1) Noble metal fission products are incorporated into the phases of the SS-15Zr alloy waste form. Several noble metals show a preference for the $Zr(Fe,Cr,Ni)_{2+x}$ intermetallic.

(2) Discrete actinide-rich phases are not seen in the SS-15Zr alloy microstructure. However, actinide-rich areas are observed within the $Zr(Fe,Cr,Ni)_{2+x}$ intermetallic.

(3) Zirconium is essential to incorporate noble metal elements in the SS-15Zr alloy microstructure. In cases where Zr is insufficient or absent, noble metal-rich phases form in the alloy.

(4) The microstructures observed in ingots prepared from irradiated hulls are similar to those observed in simulated waste forms. This suggests that the corrosion, mechanical and thermophysical properties of the radioactive ingot will be similar to those measured for the simulated MWF alloys.

## ACKNOWLEDGMENTS

The authors would like to acknowledge the U. S. Department of Energy for its support under contract W-31-109-Eng-38.

## REFERENCES

1. T.C. Totemeier and R.D. Mariani, "Morphologies of uranium and uranium-zirconium electrodeposits" , J. Nucl. Mat, **250**, (1997) p. 131-146.

2. J.J. Laidler, J.E. Battles, W.E. Miller, J.P. Ackerman, and E.L. Carls, "Development of Pyroprocessing Technology", Prog. Nucl. Energy, **31** (1997) p. 131-140.

3. J.P. Ackerman, T.R. Johnson, L.S.H. Chow, E.L. Carls, W.H. Hannum, J.J. Laidler, "Treatment of Wastes in the IFR Fuel Cycle," Prog. Nucl. Energy, **31**, (1997) p. 141.

4. S.M. McDeavitt, D.P. Abraham, J.Y. Park, and D.D. Keiser, Jr., "Stainless Steel-Zirconium Waste Forms from the Treatment of Spent Nuclear Fuel," JOM, **49** (7), (1997) p. 29.

5. D.P. Abraham, S.M. McDeavitt, and J.Y. Park, "Metal Waste Forms from the Electrometallurgical Treatment of Spent Nuclear Fuel," Proc. DOE Spent Nuclear Fuel and Fissile Management Conference, Reno, NV, June 16-20, 1996, American Nuclear Society, LaGrange Park, Illinois (1996) p. 123.

6. S.M. McDeavitt, D.P. Abraham, D.D. Keiser, Jr., and J.Y. Park, "Alloy Waste Forms for Metal Fission Products and Actinides Isolated by Spent Nuclear Fuel Treatment," Proc. Second International Symposium on Extraction and Processing for the Treatment and Minimization of Wastes: 1996, V. Ramachandran and C. C. Nesbitt, Eds., Scottsdale, AZ, October 27-30, 1996, Minerals, Metals, & Materials Society, Warrendale, Pennsylvania (1996) p. 177.

7. D.P. Abraham, S.M. McDeavitt, and J.Y. Park, Metall. Mater. Trans., **27A** (1996) p. 2151.

8. D. P. Abraham, J. W. Richardson, Jr. and S. M. McDeavitt, "Laves Intermetallics in Stainless Steel-Zirconium Alloys," Mat Sci. Eng., **A239-240**, (1997) p. 658.

9. D.D. Keiser, Jr. and S.M. McDeavitt, "Actinide-Containing Metal Disposition Alloys", Proc. DOE Spent Nuclear Fuel and Fissile Management Conference, Reno, NV, June 16-20, 1996, American Nuclear Society, LaGrange Park, Illinois (1996) p. 178.